Clinical Epigenetics

RESEARCH

Open Access

Distinct genome-wide DNA methylation and gene expression signatures in classical monocytes from African American patients with systemic sclerosis

Peter C. Allen[1,2], Sarah Smith[3], Robert C. Wilson[4], Jena R. Wirth[3], Nathan H. Wilson[3], DeAnna Baker Frost[3], Jonathan Flume[3], Gary S. Gilkeson[3], Melissa A. Cunningham[3], Carl D. Langefeld[5,6], Devin M. Absher[2] and Paula S. Ramos[3,7*]

Abstract

Background Systemic sclerosis (SSc) is a multisystem autoimmune disorder that has an unclear etiology and disproportionately affects women and African Americans. Despite this, African Americans are dramatically underrepresented in SSc research. Additionally, monocytes show heightened activation in SSc and in African Americans relative to European Americans. In this study, we sought to investigate DNA methylation and gene expression patterns in classical monocytes in a health disparity population.

Methods Classical monocytes (CD14+ + CD16−) were FACS-isolated from 34 self-reported African American women. Samples from 12 SSc patients and 12 healthy controls were hybridized on MethylationEPIC BeadChip array, while RNA-seq was performed on 16 SSc patients and 18 healthy controls. Analyses were computed to identify differentially methylated CpGs (DMCs), differentially expressed genes (DEGs), and CpGs associated with changes in gene expression (eQTM analysis).

Results We observed modest DNA methylation and gene expression differences between cases and controls. The genes harboring the top DMCs, the top DEGs, as well as the top eQTM loci were enriched for metabolic processes. Genes involved in immune processes and pathways showed a weak upregulation in the transcriptomic analysis. While many genes were newly identified, several other have been previously reported as differentially methylated or expressed in different blood cells from patients with SSc, supporting for their potential dysregulation in SSc.

Conclusions While contrasting with results found in other blood cell types in largely European-descent groups, the results of this study support that variation in DNA methylation and gene expression exists among different cell types and individuals of different genetic, clinical, social, and environmental backgrounds. This finding supports the importance of including diverse, well-characterized patients to understand the different roles of DNA methylation and gene expression variability in the dysregulation of classical monocytes in diverse populations, which might help explaining the health disparities.

Keywords Scleroderma, Autoimmune, Black, Epigenenomic, Transcriptomic, Blood

*Correspondence:
Paula S. Ramos
ramosp@musc.edu
Full list of author information is available at the end of the article

© The Author(s) 2023. **Open Access** This article is licensed under a Creative Commons Attribution 4.0 International License, which permits use, sharing, adaptation, distribution and reproduction in any medium or format, as long as you give appropriate credit to the original author(s) and the source, provide a link to the Creative Commons licence, and indicate if changes were made. The images or other third party material in this article are included in the article's Creative Commons licence, unless indicated otherwise in a credit line to the material. If material is not included in the article's Creative Commons licence and your intended use is not permitted by statutory regulation or exceeds the permitted use, you will need to obtain permission directly from the copyright holder. To view a copy of this licence, visit http://creativecommons.org/licenses/by/4.0/. The Creative Commons Public Domain Dedication waiver (http://creativecommons.org/publicdomain/zero/1.0/) applies to the data made available in this article, unless otherwise stated in a credit line to the data.

Background

Systemic sclerosis (SSc or scleroderma) is a rare, multisystem, connective tissue disease characterized by cutaneous and visceral fibrosis, immune dysregulation, and vasculopathy. SSc is very heterogeneous, with patients being commonly classified into three subsets based on the pattern of skin involvement: *sine* scleroderma, limited cutaneous SSc (lcSSc), or diffuse cutaneous SSc (dcSSc), the latter having the worse prognosis [1]. SSc is also marked by pronounced gender and ethnic disparities. Similar to other autoimmune diseases, women are four to nine times more likely to have SSc than men [2]. Relative to individuals of European descent, African Americans are more likely to develop SSc [3], have earlier onset of disease, increased disease severity, increased morbidity, earlier mortality, and reduced survival [3–12]. The etiology of SSc and the factors underlying these disparities remain elusive, and African American individuals continue to be underrepresented in research [13].

While having a family history of SSc is a risk factor for developing the disease [14], the low concordance rate of disease between monozygotic twins suggests that epigenetic and/or environmental factors may play a substantial role in SSc pathogenesis [15–17]. Indeed, genetic and epigenetic studies conducted mostly in individuals of European descent have uncovered multiple loci associated with SSc [18, 19]. Variation in DNA methylation across ancestral populations is contributed to by genetic ancestry and environmental factors [20]. Despite the increased disease burden in African Americans and variation in DNA methylation across populations, only two genome-wide differential DNA methylation analyses have been conducted in peripheral blood and skin fibroblasts from SSc patients of African descent [21, 22].

The dysregulation of monocytes in patients with SSc is well established as evidenced by their increased numbers in both peripheral blood and in skin of SSc patients [23–26] and is associated with reduced survival in SSc [26]. African Americans exhibit stronger inflammatory signatures [27–33], including heightened monocyte activation [29, 30]. As recently reviewed, monocytes are associated with altered epigenetic marks in SSc [19]. Notably, histone demethylation and chromatin dysregulation underlie monocyte dysregulation in patients with SSc [15, 34] and contribute to the trans-differentiation of fibroblasts, a key step in the pathogenesis of SSc [35, 36]. Recently, the first transcriptomic analysis of monocytes in patients with SSc revealed great variability of expression patterns across SSc patients that correlated with disease activity outcome measures [37]. The role of DNA methylation and its relationship with gene expression patterns in SSc monocytes has not been previously investigated and studies in health disparity populations are lacking.

Given the dysregulation of monocytes in SSc and the increased prevalence and severity of disease in African Americans, it is important to identify the mechanisms underlying this dysregulation and their potential contribution to the ethnic disparity. In this study, we undertook a systems-level approach, integrating DNA methylation and transcriptional data, to assess the relationship between DNA methylation and gene expression in classical monocytes from African American patients with SSc.

Results

Subject characteristics

Given the sex and ethnic disparities in SSc, this study focused on African American women, a health disparity population for SSc. All participants were self-reported African American female, and all patients met the 2013 ACR/EULAR classification criteria for SSc [38], most presenting with diffuse cutaneous SSc (dcSSc), interstitial lung disease (ILD), and being on current immunosuppressive therapies. No participants reported current infections or malignancy at the time of study visit. Additional clinical and demographic characteristics of the SSc patients and healthy controls are summarized in Table 1 and Additional File 1: Table S1, which shows the individual characteristics of the study participants. Classical monocytes (CD14++CD16-) were isolated from the study participants using fluorescence activated cell sorting (FACS).

Differentially methylated sites and genes are enriched for metabolic processes

To gain insights into functional and molecular alterations of monocytes in African American patients with SSc, over 850,000 CpG sites were tested for differential methylation between self-reported African American female patients with SSc and controls.

The differences in methylation levels between patients and controls were modest. A total of 19 differentially methylated CpGs (DMCs), which corresponds to 0.002% of all cytosines tested, meet an FDR-adjusted p value < 0.4 (Table 2). The rationale for the FDR setting was guided by the desire to perform a system-level analysis and include as many CpGs sites as possible, as well as previous studies demonstrating that this threshold permits a sensitive analysis at a system level of genes that are relevant to the underlying biology of the trait [39, 40]. A *P–P* plot of CpG association testing results supports that using $-\log(p) > 4$ is a reasonable empirical threshold of significance (Additional file 1: Fig. S1) for systems-level analyses.

In addition to CpGs near several pseudogenes, top differentially methylated CpGs included those near the genes that encode the centrosomal protein ninein (NIN, aka Glycogen Synthase Kinase 3 Beta-Interacting

Table 1 Demographic and clinical characteristics of the study participants

	DNA methylation		Gene expression	
	Patients (*n* = 12)	**Controls (*n* = 12)**	**Patients (*n* = 16)**	**Controls (*n* = 18)**
Age at enrollment (mean ± SD)	52.17 ± 12.1	48.58 ± 15.6	51.75 ± 12.3	49.28 ± 13.9
Female, *n* (%)	12 (100%)	12 (100%)	16 (100%)	18 (100%)
dcSSc, *n* (%)	6 (50%)	NA	10 (62.5%)	NA
lcSSc, *n* (%)	5 (41.7%)	NA	4 (25%)	NA
ssSSc, *n* (%)	1 (8.3%)	NA	1 (6.25%)	NA
Raynaud's Phenomenon, *n* (%)	12 (100%)	NA	16 (100%)	NA
Disease duration (mean ± SD)	11.08 ± 6.27	NA	8.88 ± 7.78	NA
mRSS (mean ± SD)[a]	13 ± 6.18	NA	13 ± 6.18	NA
ILD, *n* (%)	8 (66.7%)	NA	10 (62.5%)	NA
PH/PAH, *n* (%)	5 (41.7%)	NA	5 (31.3%)	NA
Overlap MCTD, *n* (%)	0 (0%)	NA	1 (6.25%)	NA
Overlap SLE, *n* (%)	0 (0%)	NA	1 (6.25%)	NA
Immunosuppressive medications, *n* (%)	8 (66.7%)	NA	12 (75%)	NA
Antihypertensive medications, *n* (%)	9 (75%)	NA	13 (81%)	NA
Smoker at enrollment, *n* (%)[b]	2 (16.7%)	0 (0%)	2 (12.5%)	2 (11.1%)

Immunosuppressive medications include oral steroids, mycophenolate mofetil, or hydroxychloroquine; antihypertensive medications include diuretics, calcium channel blockers, alpha blockers, beta blockers, ACE inhibitors, or angiotensin receptor antagonists

SSc systemic sclerosis, *dcSSc* diffuse cutaneous SSc, *ssSSc* sine SSc, *mRSS* modified Rodnan skin score, *ILD* interstitial lung disease, *PH/PAH* pulmonary hypertension/pulmonary arterial hypertension, *MCTD* mixed connective tissue disease, *SLE* systemic lupus erythematosus

[a] Assessed for 4 patients with dcSSc within 3–18 months of enrolment

[b] Disclosed for all participants except one control in the Gene Expression group

Table 2 Top differentially methylated CpGs between female African American patients with SSc and controls ranked by absolute effect size

CpG	Gene	Chr	Position (kb)	Relation to Island	Control *β*	SSc *β*	Difference	*p* value	Adjusted *p* value
cg22805491	NIN	14	51,172	OpenSea	0.44	0.53	0.09	2.99E−08	0.02
cg24073653	SLC41A2	12	105,221	OpenSea	0.61	0.69	0.08	2.92E−06	0.2
cg19933320	ZNF107	7	64,125	N_Shore	0.33	0.4	0.08	8.20E−06	0.35
cg06548512	LOC728989	1	146,522	Island	0.63	0.7	0.07	1.32E−07	0.05
cg00832928	SELENOT	3	150,329	Island	0.61	0.68	0.07	4.58E−07	0.11
cg08653580	CD5	11	60,862	OpenSea	0.66	0.73	0.07	1.21E−06	0.16
cg12601237	ST8SIA6	10	17,429	OpenSea	0.71	0.78	0.07	3.69E−06	0.21
cg14115740	FANCC	9	98,055	Island	0.57	0.64	0.07	4.74E−06	0.24
cg22167498	RAB11B-AS1	19	8451	N_Shelf	0.57	0.62	0.06	1.00E−06	0.16
cg23596249	MARCHF1	4	165,110	Island	0.51	0.57	0.06	1.85E−06	0.19
cg13704629	DCAF4	14	73,396	S_Shelf	0.56	0.62	0.06	2.73E−06	0.2
cg11652329	P2RX6P	22	21,399	N_Shore	0.61	0.67	0.05	4.74E−06	0.24
cg26715639	S100A11	1	151,986	OpenSea	0.6	0.65	0.05	6.43E−06	0.31
cg23493751	CCR3	3	46,205	OpenSea	0.75	0.8	0.05	7.64E−06	0.34
cg08288426	ZSCAN29	15	43,651	OpenSea	0.8	0.76	− 0.04	1.51E−06	0.17
cg18507060	OAS3	12	113,399	OpenSea	0.77	0.81	0.04	5.48E−07	0.11
cg10044900	CFAP44	3	113,058	OpenSea	0.76	0.8	0.04	2.55E−06	0.2
cg14929421	ACTR3BP2	2	92,318	OpenSea	0.52	0.55	0.03	2.80E−06	0.2
cg04331667	CCDC71L	7	106,171	OpenSea	0.8	0.83	0.03	3.21E−06	0.2

CpGs are shown, along with nearest gene, annotation, averaged methylation levels (*β*), methylation difference, unadjusted and adjusted *p* values

Protein), the selenoprotein T (SELENOT), the synthetase OAS3, or the melanoprotein T-Cell Surface Glycoprotein CD5 (Table 2; Additional file 1: Figs. S2 and S3).

We sought to investigate any potential enrichment (or conversely, underrepresentation) of DMCs in defined genomic regions (Fig. 1). Among the top 100 DMCs, there was an overrepresentation of DMCs in exon boundaries (OR = 4.9, $p < 0.0001$), while there was a depletion of DMCs in the vicinity of transcription start sites (OR = 0.2, $p < 0.005$).

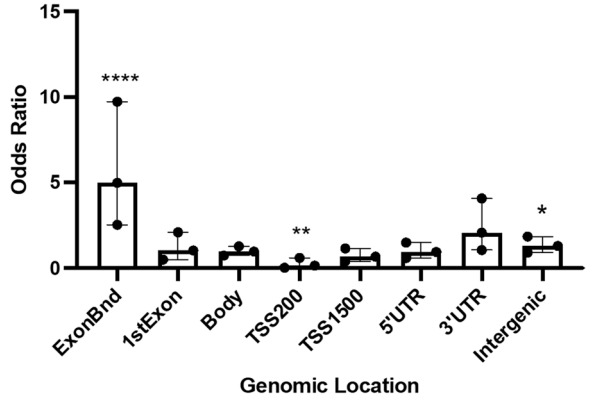

Fig. 1 Genomic location of the top 100 differentially methylated CpGs (DMC). Odds ratio (OR), 95% confidence intervals (CI), and *p* values were computed against the general distribution of the CpGs using GraphPad Prism v9. Error bars represent the 95% CI. OR indicates the enrichment or depletion of DMCs in each region. *$p < 0.05$; **$p < 0.005$; ****$p < 0.0001$. TSS: transcription start site. TSS200: 0–200 bases upstream of the transcriptional start site (TSS). TSS1500: 200–1500 bases upstream of the TSS

To better understand the chromatin context and functional role underlying the disease-associated CpG sites, we performed integrative epigenomics analyses using the eFORGE 2.0 framework [41–43] to assess whether these SSc-associated CpGs reside within regulatory regions across the genome in diverse tissues and cell types. Using the top 100 DMCs associated with SSc showed an enrichment of H3K9me3 (a histone mark associated with heterochromatin regions, important for repressing repetitive elements, non-coding portions of the genome, and silencing lineage-inappropriate genes) in several fetal cells (blue in Fig. 2), and an enrichment of H3K36me3 (a transcription-associated histone mark important in maintaining gene expression stability and regulation of DNA damage repair) in several blood, stem and fetal cells (pink in Fig. 2). Overall, these findings suggest that most epigenetic changes are present in non-transcribed regions.

We first used the DAVID Functional Annotation Tool 6.8 [44, 45] to uncover the biological significance of the genes in the regions of the differentially methylated cytosines shown in Table 2. Although not significant, the top Gene Ontology (GO) terms were related to Metabolic Processes (GO:0008152; $p = 0.4$), driven by OAS3, DCAF4, FANCC, S100A11, ST8SIA6, RNF24, SELENOT, ZSCAN29, and ZNF107. Close to half of the genes harboring DMC are phosphoproteins:

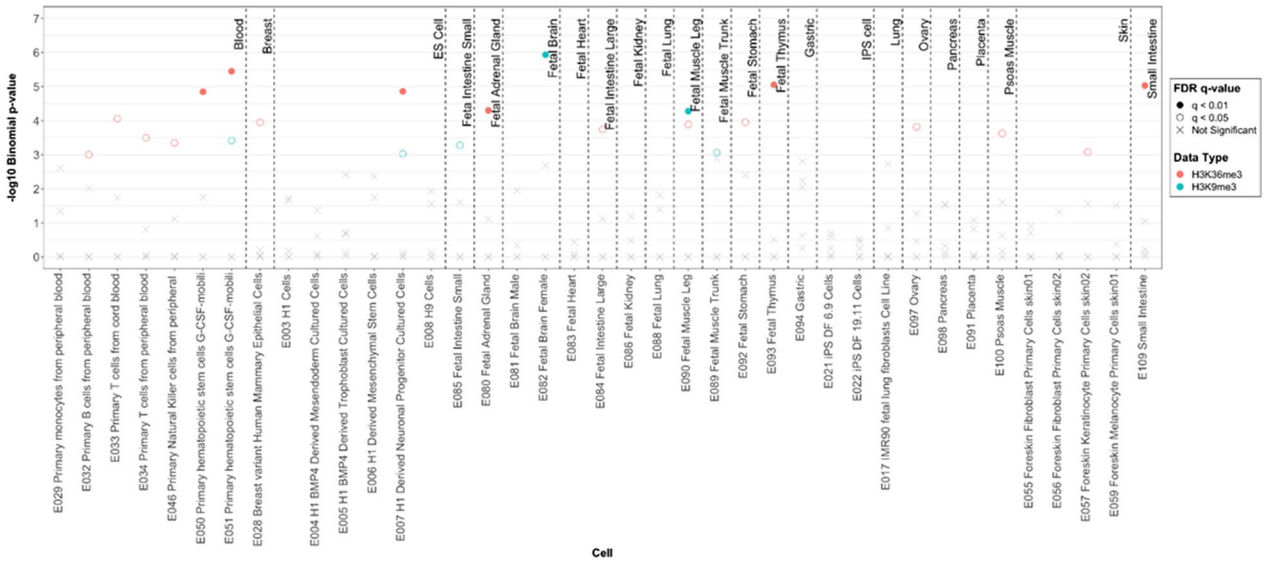

Fig. 2 Enrichment of differentially methylated CpGs in H3K9me3 and H3K36me3 histone marks among various cell and tissue types using Roadmap Epigenomics project data. Statistically significant enrichment outside the 99.9th percentile (− log10 binomial *p* value ≥ 3.38) is colored red on the vertical axis

OAS3, CCR3, S100A11, CFAP44, CCDC71L, SLC41A2, ZSCAN29, CD5, NIN.

Next, we used *Enrichr* [46, 47] to explore the Biological Processes and KEGG pathways associated with the genes harboring the top DMCs in Table 2. As shown in Fig. 3, the top Biological Processes were related to metabolic processes, including those of RNA (GO:0060700, $p = 4.9E{-}03$ (driven by the ribonuclease OAS3)) and protein (GO:0032069, $p = 5.9E{-}03$ (driven by the selenocysteine SELENOT)) metabolic processes, as well as hormone secretion (GO:0060124, $p = 5.9E{-}03$ (driven by OAS3 and SELENOT)). No pathways showed significant enrichment.

Differentially expressed genes are enriched for metabolic processes

Differential gene expression analysis revealed a total of 1272 transcripts differentially expressed between African American female patients with SSc and controls at an FDR-corrected $p < 0.4$ (Additional file 1: Fig. S4). These differentially expressed transcripts correspond to 5.0% of all 25,369 transcripts tested. The rationale for the FDR setting was the same as described above for the DNA methylation analysis. The top differentially expressed transcripts are shown in Table 3.

The top differentially expressed genes (DEGs) include the collagen *COL9A2*, the endoplasmic reticulum transmembrane channel-like *TMC8* gene, the heparinase *HPSE*, the proto-oncogene nuclear ubiquitin ligase *MDM2*, the vesicular trafficking cytohesin *CYTH4*, the phospholipase *PLD1*, and the Kruppel-like transcription factor *KLF6* (Table 3).

Gene Ontology analysis of the top transcripts (Table 3) using DAVID 6.8 showed many genes that participate in metabolic processes (GO:004423; $p = 2.70E{-}02$ (KLF6, MDM2, SMARCA4, ABHD5, GDAP1, HPSE, HIVEP3, INSIG2, IVD, KYNU, OBSCN, PLD1, POT1, PPP1R14B, RNF146, SLC35B3, ZNF654)), especially catabolic processes (GO:0044248; $p = 2.0E{-}02$ (MDM2, ABHD5, HPSE, IVD, KYNU, PLD1, RNF146), and sulfur compound metabolic process (GO:0006790; $p = 8.0E{-}03$ (GDAP1, HPSE, KYNU, SLC34B3)).

Enrichr analysis of the top differentially expressed genes in Table 3 revealed an enrichment of several biological processes related to metabolic processes (e.g., GO:0006654, $p = 1.0E{-}03$), as well as an enrichment of the KEGG endocytosis pathway ($p = 1.9E{-}03$) (Fig. 4A and B). Relaxing the threshold and including the 450 transcripts with FDR-corrected $p < 0.3$ in the comparison between cases and controls revealed an involvement of immune biological processes and pathways (Fig. 4C, D).

Expression quantitative trait methylation (eQTM) analysis

To investigate the potential mechanistic relationship between DNA methylation and gene expression variation in classical monocytes, we leveraged RNA-sequencing data from the same individuals and computed an expression quantitative trait methylation (eQTM) analysis to identify CpGs associated with changes in gene expression. Table 4 shows the top eQTM loci, which include the transcriptional repressor homolog *PCGF1*, the

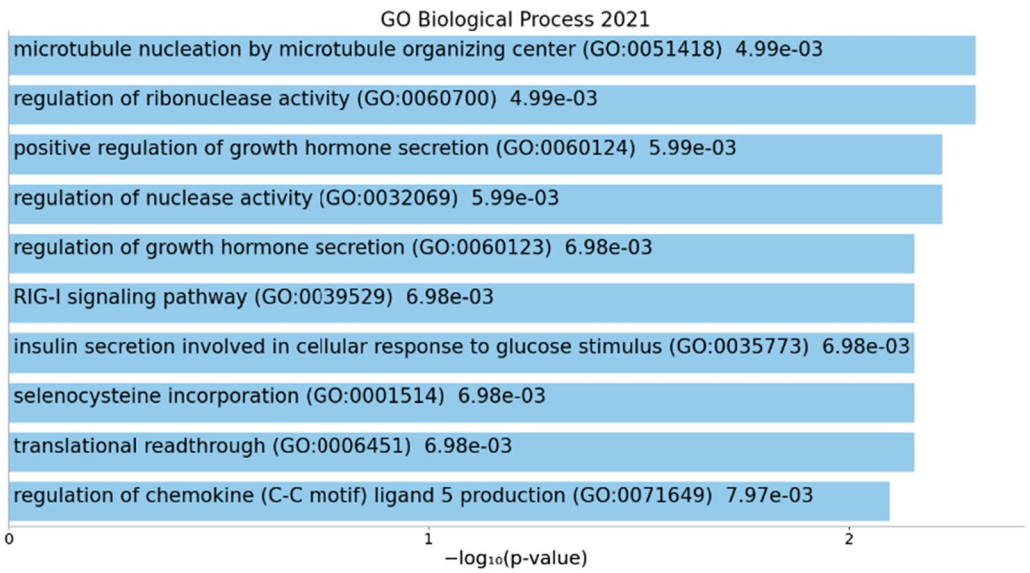

Fig. 3 Metabolic process enrichment among the genes harboring the top DMCs. The x-axis shows the − log10(*p* value) of the Biological Process enrichment obtained from Enrichr. The length of the bar represents the significance of that specific term

Table 3 Top 20 differentially expressed transcripts between female African American patients with SSc and controls ranked by absolute effect size

Gene	Chr	Start (kb)	End (kb)	Strand	logFC	logCPM	*p* Value	Adjusted *p* value
COL9A2	1	40,766	40,883	−	−1.18	3.04	1.26E−04	0.25
OBSCN	1	228,296	228,495	+	−1.13	2.13	5.01E−04	0.25
PPP1R14B	11	64,012	64,114	−	−0.65	2.53	2.17E−04	0.25
GDAP1	8	75,163	75,279	+	0.57	4.1	3.66E−04	0.25
TMC8	17	76,027	76,139	+	−0.54	6.38	5.50E−05	0.25
ZNF654	3	88,088	88,194	+	0.43	4.19	2.37E−04	0.25
KYNU	2	143,535	143,735	+	0.43	7.52	3.25E−04	0.25
KLF6	10	3818	3927	−	0.42	9.52	1.94E−04	0.25
INSIG2	2	118,746	118,868	+	0.41	3.65	2.79E−04	0.25
SLC35B3	6	8,413	8,536	−	0.41	4.39	3.10E−04	0.25
POT1	7	124,470	124,670	−	0.41	4.64	4.27E−04	0.25
HIVEP3	1	42,284	42,484	−	−0.4	5.13	2.65E−04	0.25
HPSE	4	84,216	84,356	−	0.4	6.6	6.95E−05	0.25
MDM2	12	69,102	69,239	+	0.37	7.08	1.42E−04	0.25
ABHD5	3	43,632	43,764	+	0.36	5.8	4.49E−04	0.25
RNF146	6	127,488	127,610	+	0.36	5.85	4.66E−04	0.25
IVD	15	40,598	40,714	+	−0.34	5.67	2.20E−04	0.25
SMARCA4	19	10,972	11,172	+	−0.31	7.93	2.97E−04	0.25
PLD1	3	171,428	171,628	−	0.27	5.99	1.78E−04	0.25
CYTH4	22	37,578	37,711	+	−0.26	7.88	1.71E−04	0.25

Genes are shown, along with location, strand, logarithm fold change (logFC), logarithm of counts per million reads (logCPM), unadjusted and adjusted *p* values

RNA helicase *DDX27*, and the splicing factor *SF3B2*. About half the eQTM loci showed a negative correlation between DNA methylation and gene expression levels, while the other half displayed a positive correlation (Table 4).

These 25 genes whose expression is associated with DMCs are enriched for cellular metabolic processes according to DAVID (GO:0044237, $p = 6.50E{-}03$ (driven by BCR, DDX27, DDX41, E2F4, MLLT6, PBX2, RAB11B, U2AF2, CHD1, DCTPP1, ITPKB, KYNU, MMP9, PCGF1, RNF123, SF3B2, TDP2, UBR3)). In addition to microtubule cytoskeleton organization processes, other metabolic processes like RNA splicing and processing were also unveiled by Enrichr (Fig. 5). The top KEGG Pathway was vasopressin-regulated water reabsorption (Fig. 5).

Discussion

This study is to our knowledge the first to evaluate and integrate analysis of DNA methylation and gene expression in classical monocytes from African American patients with SSc on a genome-wide scale. We show modest differences in DNA methylation and gene expression between patients and controls, and an enrichment of genes involved in metabolic processes.

The differential methylation analysis showed that the top DMCs were enriched for H3K9me3 and H3K36me3, markers associated with heterochromatic regions in several fetal tissues. This is consistent with the recent finding that several tissue-specific repressed genomic regions are enriched for disease-associated GWAS variants, and suggests that DMC may also have tissue-specific effects in repressive regions [43]. Previous analyses of DNA methylation in other blood cell types and in largely European-descent groups [21, 48–53] report a larger difference in DNA methylation patterns between cases and controls, and an enrichment of genes involved in immune and inflammatory processes. In our study, only *OAS3* and *CD5* have been previously reported as differentially methylated in CD4 + T cells from Spanish patients with SSc [53]. OAS3 is an interferon-induced, dsRNA-activated antiviral enzyme which plays a role in cellular innate antiviral response and the immune response to the interferon pathway [54, 55]. Its expression can be increased in SSc patients [56]. CD5 is a type-I transmembrane glycoprotein found on the surface of thymocytes, T lymphocytes, and a subset of B lymphocytes. CD5 is upregulated in B cells from patients with SSc [57]. Among other genes harboring top DMCs, the centrosomal protein NIN has a role in promoting angiogenesis

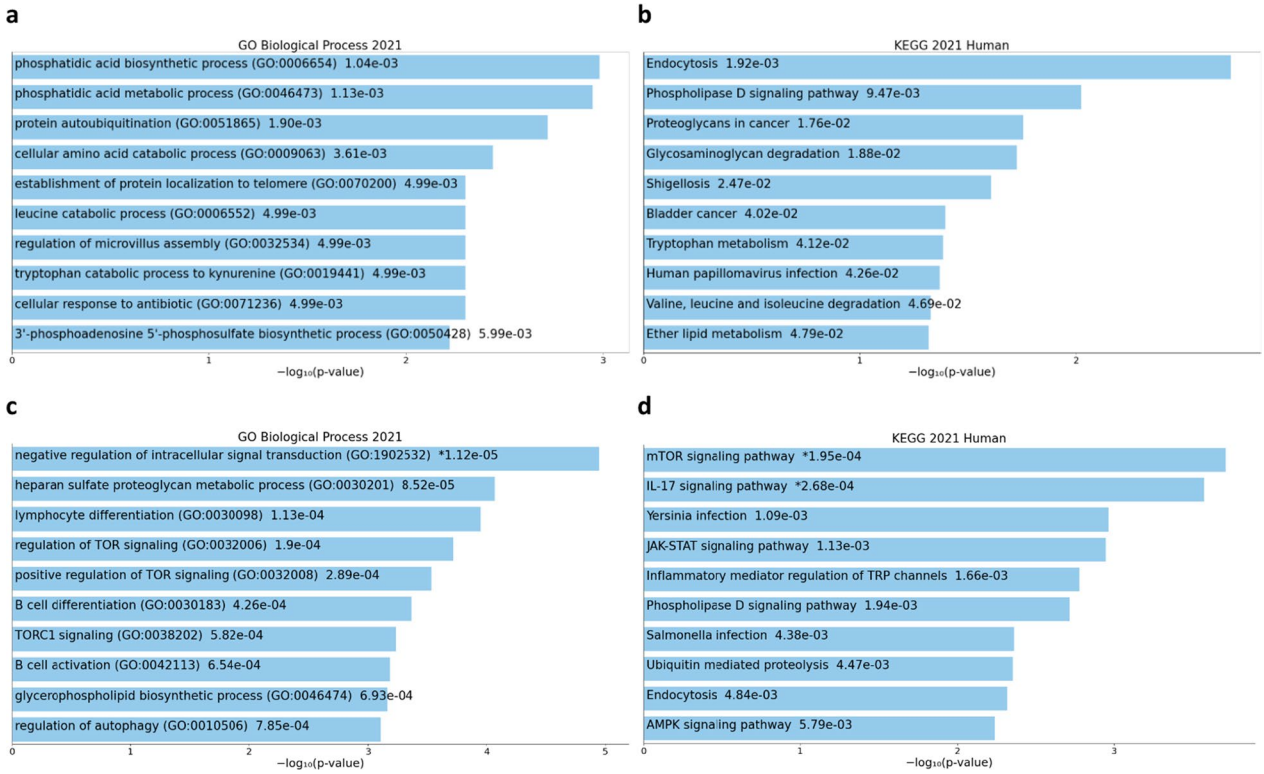

Fig. 4 Metabolic and immune process and pathway enrichment among differentially expressed genes. Biological processes (**a**) and KEGG pathways (**b**) enriched for the top 20 DEG; biological processes (**c**) and KEGG pathways (**d**) enriched for the top 450 DEG. The x-axis shows the − log10(*p* value) of enrichment obtained from Enrichr. The length of the bar represents the significance of that specific term

[58], which is dysregulated in SSc. Antibodies against NIN are present in sera from several patients with SSc and other autoimmune disorders [59], which further supports a role for NIN in SSc. Interestingly, NIN may also be regulated by GSK-3β, a key regulator of the canonical Wnt signaling in fibroblasts whose inhibition results in fibroblast activation and increased release of collagen [60].

Multiple analyses of gene expression patterns in different blood cell types from mostly European-derived populations consistently report a prominent upregulation of genes involved in immune and inflammatory processes in SSc patients [37, 61–74]. This includes the only analysis of classical monocytes to date [37] and contrasts with the weaker upregulation of inflammatory and immune genes we observed in classical monocytes from African American SSc patients. Multiple DEGs found in our analysis have been previously reported as differentially expressed in different blood cells from patients with SSc, including the endoplasmic reticulum transmembrane channel-like *TMC8* [53], the collagen *COL9A2* [66], the Kruppel-like transcription factor *KLF6* [37, 53, 61], the zinc finger ZNF654 [53], the insulin-Induced INSIG2 [53], the transcription regulator SMARCA4 [53], the kynureninase *KYNU* [37, 62, 63, 68], the telomere regulator POT1 [53], and the hydrolase *ABHD5* [63, 68]. However, when we focus on classical monocytes, our results are consistent in significance and directionality of effect to those reported by Makinde and colleagues for *HPSE, CYTH4, KLF6, KYNU, C6orf62, and TUBB4B* [37], providing support for their potential dysregulation in SSc.

The variable correlation between methylation patterns and gene expression is well established, being either positive or negative, and being tissue and context specific, in that the local DNA sequence and genomic features largely account for local patterns of methylation [33, 75–81]. In our eQTM analysis, we found that about half of the DMCs have a positive and half a negative correlation with gene expression levels. Several of the genes whose expression was associated with eQTM have been previously reported as differentially expressed in different blood cells from patients with SSc, lending further support for their dysregulation in SSc patients. These include DDX27 [53], C6orf62 [53], CHD1 [65], BCR [53], TDP2 [53], MLLT6 [53], RAB11B [53], CLIP4 [53], PBX2 [53], MMP9 [70], and KYNU [37, 62, 63, 68].

Our results provide support for the involvement of dysregulated metabolic processes in SSc, consistent with

Table 4 Top 25 eQTM loci

CpG Gene	CpG	CpG Chr	Position (kb)	Transcript Gene	Coefficient	*p* value
CCDC142	cg00402980	2	74,701	PCGF1	191.93	0.001
CSE1L	cg06719602	20	47,696	DDX27	−111.63	0.001
CFL1	cg03252697	11	65,623	SF3B2	−682.91	0.005
CCDC142	cg00402980	2	74,701	DCTN1	−892.47	0.011
KIAA0895L	cg10031648	16	67,211	E2F4	−126.96	0.028
KIAA0319	cg11457367	6	24,646	C6orf62	849.33	0.036
LOC100289230	cg16525244	5	98,273	CHD1	656.51	0.062
IP6K1	cg27076861	3	49,762	RNF123	−270.99	0.068
KLHDC10	cg02630604	7	129,782	KLHDC10	203.05	0.093
BCR	cg23436282	22	23,665	BCR	−153.94	0.106
KIAA0319	cg11457367	6	24,646	TDP2	193.28	0.111
PCGF2	cg18826743	17	36,901	MLLT6	−205.72	0.114
B4GALT7	cg05174883	5	177,038	DDX41	126.69	0.122
RAB11B-AS1	cg22167498	19	8,451	RAB11B	−45.50	0.135
ITPK1	cg21166544	14	93,604	BTBD7	54.13	0.166
ZNF628	cg12450907	19	55,993	U2AF2	−61.93	0.200
PCARE	cg20836546	2	29,298	CLIP4	299.96	0.209
ACADSB	cg07971827	10	124,772	FAM24B	−4.48	0.241
GIMAP7	cg01444712	7	150,211	GIMAP2	200.96	0.248
ITPKB	cg22444124	1	226,868	ITPKB	−122.24	0.277
NOTCH4	cg26950898	6	32,164	PBX2	−275.47	0.387
CD40	cg06282353	20	44,738	MMP9	513.29	0.412
METTL5	cg02173085	2	170,678	UBR3	123.62	0.419
KYNU	cg11805548	2	143,634	KYNU	209.42	0.422
ZNF768	cg01174674	16	30,543	DCTPP1	9.04	0.430

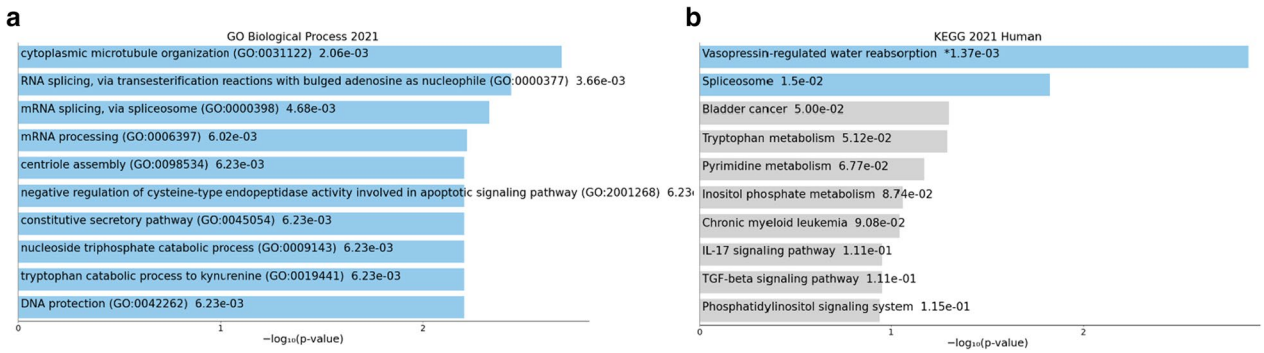

Fig. 5 Biological processes (**a**) and KEGG pathways (**b**) enrichment among genes associated with eQTM loci. The x-axis shows the − log10(*p* value) of enrichment obtained from Enrichr. The length of the bar represents the significance of that specific term. Terms displayed in gray are not significant

previous studies, reporting that dysregulated metabolism is associated with SSc [82]. Different metabolic perturbations are expressed in different patients, reflecting the clinical heterogeneity of SSc [82]. Our enrichment of genes involved in metabolic processes contrasts with the prominent enrichment of genes involved in immune and inflammatory processes consistently reported in both DNA methylation [21, 48–53] and gene expression analyses in multiple blood cell populations and in largely European-descent groups [37, 61–74]. This is not surprising, given that previous studies have focused on blood (a heterogeneous tissue) or lymphoid cell populations, while our focus was on a myeloid cell population. The distinct racial category of the participants might appear

as another explanation for this difference. However, we caution against a simplistic explanation solely based on self-reported race. Race is an imperfect proxy for social determinants of health such as racism and discrimination, economic stability, healthcare access and quality, education access, and environmental exposures. These social and environmental determinants are differentially experienced across groups and geography, resulting in health disparities. We postulate that these sociocultural factors experienced by our study participants are one of the reasons underlying our results. The other reason that can explain the lack of replication across populations is genetic ancestry. Differences in DNA methylation are known to exist between individuals of African and European ancestry [20, 27, 33, 83–87], due to both variation in genetic ancestry and environmental factors [20]. These differences help explain the new findings and minimal overlap with previous reports.

Several other reasons and important limitations of this study might underlie the modest differences in DNA methylation and gene expression we observed in our study focused on classical monocytes from self-reported Black women. First, although this study is the first to evaluate DNA methylation and gene expression patterns in monocytes of African Americans, the sample size is very small. This study has virtually no power to detect the DNA methylation differences herein reported, but is powered to detect a reasonable fraction of the differentially expressed transcripts between cases and controls. Nevertheless, with 16 total SSc cases, it is comparable to sample sizes from previous studies that assessed genome-wide DNA methylation and gene expression primarily in European Americans [15, 37, 88, 89]. Also, our results are consistent with the heightened monocyte activation previously reported in African American patients with SSc [29, 30].

Second, we do not have DNA available on these study participants to allow us to estimate their genetic ancestries, and this study relies on self-reported race. Although we observed no evidence of population structure and adjusted for population stratification, to mitigate against the limitations of this study it is essential that future studies genotype and including multiple African groups to fully capture African genetic diversity.

Third, SSc is a rare disease with a prevalence of only 49,000 US adults [90], and there is currently no existing cohort or repository of samples from African American patients that can be leveraged to enable large-scale studies, to replicate, and to validate our results. Given our small sample size, we tried to balance our desire to increase discovery at the cost of additional loci being false positive results, which is a reasonable premise to pursue systems-level analyses.

Fourth, most of the patients in our study presented with more severe SSc and were on current immunosuppressive therapies that can impact their epigenetic and transcriptional patterns. Although the modest sample size of this study precludes a robust statistical adjustment for immunosuppressive drug use, and these medications affect the methylation levels of several CpGs, we also show that their use does not cause a substantial bias in our study (Additional file 1: Figs. S6 and S7). Interestingly, in their transcriptional analysis of classical monocytes in SSc patients, Makinde et al. [37], which included participants of different self-reported racial groups, note the substantial variability in the transcriptional profiles of the patients, with several patients, especially those on current immunosuppressive therapies, more closely resembling controls. This observation is consistent with our results where African American patients, who tend to have more severe disease and be on immunosuppressants, show modest differences in gene expression relative to controls.

Fifth, and inherent to all epigenomic studies, we cannot exclude the possibility of reverse causation, or whether the DNA methylation and gene expression changes are a cause or an effect of SSc. Future longitudinal studies will help to elucidate the role of DNA methylation in disease etiology. Sixth, it is possible that the DNA methylation changes are due to genetic variation, but we lack genotypic data on these samples. Seventh, SSc is a very heterogeneous disorder, which can also explain the inconsistent and sometimes disparate results observed in different studies, including the lack of association between gene expression signatures and clinical characteristics [91, 92]. Similarly, African Americans are a heterogeneous category of individuals with diverse cultural and genetic backgrounds [93].

Finally, we recognize that it is difficult to account for all lifestyle factors that could affect DNA methylation [17]. Unless studies account for all the genetic, clinical, demographic, behavioral, social, and environmental characteristics of their participants, limited reproducibility is not unexpected. Future studies including diverse individuals with measures of genetic ancestry as well as environmental and social determinants of health responsible for the health disparities will ensure the validity and relevance of these findings for patients of all backgrounds. Despite these limitations, the findings in this study further support the need to continue to investigate the regulatory architecture of different cell types in diverse SSc patients.

Conclusions

Our study suggests that classical monocytes from African American female patients with SSc display modest changes in DNA methylation and gene expression

relative to healthy controls. The genes associated with the DMCs, DEGs, as well as eQTM loci, show an enrichment of metabolic processes, and only a weak upregulation of immune processes and pathways. These differences relative to previous reports of differential methylation and gene expression in patients with SSc epitomize the clinical, biological, social, and environmental heterogeneity of SSc patients. This study underscores the importance of research in patients with diverse clinical and sociodemographic characteristics, and of integrating genetic and social factors, to enable a thorough understanding of the different roles of DNA methylation and gene expression variability in the dysregulation of classical monocytes in different populations.

Methods

Subjects

A total of 34 self-reported Black or African American females were recruited for this study: 16 patients with SSc and 18 healthy controls. All patients met the 2013 ACR/EULAR classification criteria for SSc [38]. Cases and controls were age-balanced within 5 years.

Classical monocyte isolation

Peripheral blood (40 ml) was drawn by venipuncture into EDTA tubes and stored at 4 °C overnight. Peripheral blood mononuclear cells (PBMCs) were isolated using Sep-Mate tubes and Lymphoprep (Stem Cell Technologies, Cambridge, MA, USA) according to manufacturer guidelines. After isolation, any residual red blood cells were depleted via red blood cell lysis (144 mM NH_4Cl and 17 mM Tris, pH 7.6), washed twice with 1X PBS, and stored at − 80 °C in 90% Fetal Bovine Serum (FBS)/10% dimethyl sulfoxide (DMSO). After thawing, PBMCs were stained with CD-14 Brilliant violet 421 (1:100) and CD-16 Brilliant violet 605 (1:100). Cells were incubated with antibodies for 30 min on ice in the dark. Both antibodies were purchased from Biolegend (San Diego, CA, USA). Viability was assessed using Near-infrared Live/Dead Fixable Dead Cell stain (Life Technologies, Carlsbad, CA, USA) at a concentration of 50 µl/million cells. CD14++/CD16- cells were collected with a FACSAria III cell sorter (BD Biosciences, San Jose, CA, USA).

MethylationEPIC assays, quality control and batch normalization

DNA was extracted using DNeasy kits (Qiagen, Germantown, MD, USA) according to manufacturer protocols from classical monocytes (CD14++CD16-) isolated from 12 female African American SSc patients and 12 female African American controls. DNA methylation was assessed using Illumina's MethylationEPIC BeadChip (Illumina, San Diego, CA, USA). 500 ng of each sample was bisulfite converted using an EZ DNA Methylation Kit (Zymo, Tustin, CA, USA), amplified, hybridized and imaged. DNA methylation data for over 850,000 CpGs were generated per sample and preprocessed using GenomeStudio in the form of beta values, which is the estimate of the proportion of methylation in a cell population. GenomeStudio also produced detection p values, which is the probability that the intensity is due to background noise rather than a true signal. After filtering out background noise, ComBat [94] was used as an empirical Bayes approach to correct for differences between batches. A single array containing 12 samples and approximately 20,000 CpGs separated at random was used to describe a batch to be normalized on our in-house, high-performance computing cluster at the HudsonAlpha Institute for Biotechnology. After correcting for batch effects, beta values between the two probe types, Infinium I & Infinium II, were normalized by using the equation: $\text{Beta}_{\text{Type II Probe}} = Y + \beta_1 \times \text{Beta}_{\text{Type II Probe}} + \beta_2 \times \text{Beta}^2_{\text{Type II Probe}}$. The intercept and beta coefficients were calculated by fitting a second-order polynomial to beta values from paired Infinium I and Infinium II CpGs that were within 50 bp of each other as described previously [95].

Only good quality samples (successful probe ratio > 0.1) were included. CpG probes with detection p values over 0.01 were removed. The R package ChAMP [96] was used to exclude non-CpG probes, probes that have been previously reported to bind to multiple locations [97], and probes with a bead count less than 3 in ≥ 5% of samples per probe.

Given the lack of genetic ancestry estimates, we used EPISTRUCTURE, a method for the inference of ancestry from methylation data that relies on reference data in which both genotype and methylation data are available [98]. The PCA plot generated using EPISTRUCTURE shown in Additional file 1: Fig. S5 shows no evidence of population structure. Smoking is known to affect methylation across the genome; therefore, CpGs known to be associated with smoking were removed prior to analysis [99]. After pre-processing and filtering of the methylation data, 817,938 CpGs remained for downstream analysis. Genome-wide data methylation analysis was then performed using the R statistical suite (version 3.6.3) [100]

Genome-wide DNA methylation regression analysis

Linear regression analyses were performed at each CpG using the stats package in R [100] to test whether that particular CpG was associated with SSc by examining DNA methylation differences between patients and controls. Principal components were calculated using the built-in R function prcomp() from the stats package and

used in our regression model to correct for unknown potential sources of variance such as admixture. In our model, disease status was considered the random effect, and the first two principal components were considered fixed; due to age being known to influence DNA methylation, it was also placed as a covariate:

$$\text{Methylation Beta Value} \sim \beta_1 \times \text{Disease Status} + \beta_2 \times \text{Age at Collection} + \beta_3 \times \text{PC1} + \beta_4 \times \text{PC2} + \varepsilon$$

The associated CpG p values were then corrected using the Benjamini–Hochberg False Discovery Rate (FDR) method. Given the paucity of differentially methylated cytosines identified with FDR-corrected $p < 0.05$, cytosines with an FDR-corrected $p < 0.4$ are reported. The rationale for the FDR setting was guided by the desire to perform a system-level analysis and include as many CpGs sites as possible, as well as previous studies, demonstrating that this threshold permits a sensitive analysis at a system level of genes that are relevant to the underlying biology of the trait [39, 40]. The premise that most CpGs have sufficient quality, coupled with the desire to increase discovery at the cost of additional loci being false positive results, is a reasonable premise for initial studies to pursue pathway and network analyses. To further select an empirical threshold for significance using a data-informed approach, we generated the *P*–*P* plot to see the point of departure where the CpGs start deviating from the null (Additional file 1: Fig. S1). As shown in Additional file 1: Fig. S1, fitting a linear regression line for the theoretical domain of $0 < \text{theoretical} - \log(\text{p}) < 3$ and extrapolating line beyond 3 suggests that the line departs from fitting the empirical $-\log(p)$ data approximately at 4. Thus, $-\log(p) > 4$ is a reasonable empirical threshold for significance for system level analyses.

To minimize confounding due to smoking, the 3348 CpGs reported as associated with smoking in Christiansen et al. [99] were removed. This included CpGs replicated in American Indian and African American samples. Another potential confounder on the DNA methylation patterns is the use of immunosuppressive therapies by most patients with SSc. Given the small sample size of this study and the potential risk of overfitting if adjusting for immunosuppressive use, we show instead that the use of immunosuppressive therapies does not heavily bias the association results, although there are several CpGs that show meaningful increases in beta coefficients due to immunosuppressive medication use (Additional file 1: Figs. S6 and S7). The top three CpGs most significantly associated with SSc among immunosuppressive users include cg22196946 in the 5′UTR near *IL15*, cg22187722 in the 5′UTR near *CPVL*, and cg17710334 in an intergenic region. None of these CpGs reaches the empirical threshold for significance among all SSc patients (Additional file 1: Fig. S7).

The power evaluation tool pwrEWAS was used to estimate power as a function of sample size and effect size ($\Delta\beta$) for two-group comparisons of DNAm assessed using Illumina Human Methylation BeadChip technology [101]. For a total number of 24 subjects (1:1 case/control ratio), and using liver as a proxy for a homogeneous cell population, this study has 4% power to detect differences in up to 6% in CpG-specific methylation across 20 CpGs between groups (the median DNA methylation difference between averaged methylation levels between cases and controls reported in Table 2), and 6% power to detect differences in up to 8% in CpG-specific methylation across 20 CpGs between groups (the maximum DNA methylation difference between averaged methylation levels between cases and controls reported in Table 2). Hence, this study is not powered to detect the DNA methylation differences reported in Table 2.

Associated CpGs identified as significant at FDR-corrected $p < 0.4$ were used to identify the closest gene, and then, those genes were analyzed for common pathways and functions. Given the limited statistical power, exploratory analysis of clinical features was not computed.

RNA sequencing

Total RNA was extracted from classical monocytes isolated from 16 female African American patients and 18 female African American controls using the RNeasy Kits (Qiagen, Germantown, MD, USA) according to the manufacturer's guideline. RNA integrity (RIN) was verified on an Agilent 2200 TapeStation (Agilent Technologies, Palo Alto, CA, USA). The RIN values ranged from 1.8 to 9.0 with an average RIN of 5.8. Due to the low RIN, RNA sequencing libraries were prepared using Illumina's TruSeq RNA Exome kit. Total RNA (40 ng) of was used to prepare RNA-Seq libraries following the protocol as described by the manufacturer (Illumina, San Diego, CA, USA). Libraries were clustered at a concentration to ensure an average of 25 million reads per sample on the cBot as described by the manufacturer (Illumina, San Diego, CA, USA). Clustered RNA-seq libraries were single read sequenced using version 4 with 1X50 cycles on an Illumina HiSeq2500. Demultiplexing was performed utilizing bcl2fastq- v2.19 to generate Fastq files.

Gene expression analysis

Upon sequencing, data were analyzed by Rosalind, with a HyperScale architecture developed by OnRamp BioInformatics. Individual sample reads were aligned to the hg19 reference genome using STAR and quantified using HTseq. The subsequent transcript data were imported

into R and the edgeR package used to preprocess the data. The transcript counts were normalized using the trimmed mean of M values (TMM) method. To account for potential non-biological variance in the gene expression data, a quasi-likelihood negative binomial generalized log-linear model [102] was used and the data tested for differential expression. FDR p values were then calculated for each transcript. Since no differentially expressed transcripts were identified with FDR-corrected $p<0.05$, an FDR-corrected $p<0.4$ was used. The rationale for the FDR setting was guided by the desire to perform a system-level analysis and include as many transcripts as possible, as well as previous studies demonstrating that this threshold permits a sensitive analysis at a system level of genes that are relevant to the underlying biology of the trait [39, 40].

RNASeqPower (version 1.39.0) was used to estimate the power given 16 cases and 18 controls, coverage depth (25 M reads) and a coefficient of variation of 0.4 as recommended for human samples and equivalent across groups [103]. Using an $\alpha=0.0001$, which based on our experience is a a good approximation to a FDR = 0.05, this study has 9%, 70%, and 97% power to detect differential expression or fold change (FC) of 1.5, 2.0, and 2.5 or higher, respectively. These FC correspond to logFC > |0.18|, logFC > |0.30|, and logFC > |0.40|, respectively. Given the median logFC ~ |0.40|, this study is powered to detect a reasonable fraction of the differentially expressed transcripts between cases and controls.

Expression quantitative trait methylation (eQTM) analysis

To identify associations between DNA methylation levels and gene expression of nearby genes, a linear regression model was created using the top CpGs and transcripts from both analyses, ranked by unadjusted p value. A total of 1272 differentially expressed transcripts that met an FDR-corrected $p<0.4$ were used for this analysis. To correct for unknown sources of variation in the methylation beta scores (e.g., admixture, cellular contamination), the effects of the first two principal components were regressed out and the residuals used in downstream analysis. To correct for the variation in the RNA-seq data, the data were normalized using the TMM. CpGs within 100 kb of the transcript start or end positions were associated with the respective transcript. The RNA transcript was considered the random effect, and the methylation beta value and age of the patient were considered the fixed effects:

$$\text{Transcript Value} \sim \beta_1 \times \text{CpG Beta Score} + \beta_2 \times \text{Age at Collection} + \varepsilon$$

Functional annotation enrichment analysis

The position of each CpG was annotated to the corresponding genomic location as provided by Illumina (TSS1500, TSS200, 5′ UTR, 1st Exon, Body, Exon boundaries, 3′ UTR, and intergenic). To investigate the distribution of differentially methylated CpGs (DMC) in different genomic locations, the top 100 CpGs were used to compare their localization in different genomic locations. Odds ratio (OR), 95% confidence intervals (CI), and p values were computed against the general distribution of all CpGs of our dataset using GraphPad Prism (version 9.3.1). For regulatory annotation of the differentially methylated CpGs, eFORGE v2.0 (https://eforge.altiusinstitute.org/) [41–43] was used to identify if the associated CpGs were enriched in cell-specific regulatory elements, namely DNase I hypersensitive sites (DHSs) (markers of active regulatory regions) and loci with overlapping histone modifications (H3Kme1, H3Kme4, H3K9me3, H3K27me3, and H3K36me3) across available cell lines and tissues from the Roadmap Epigenomics Project, BLUEPRINT Epigenome, and ENCODE (Encyclopedia of DNA Elements) consortia data. Both the top 100, as well as the top differentially methylated CpGs that met an FDR-adjusted $p<0.4$, were entered as input of the eFORGE v2.0 analysis and tested for enrichment for overlap with putative functional elements compared to matched background CpGs. The matched background is a set of the same number of CpGs as the test set, matched for gene relationship and CpG island relationship annotation. One thousand matched background sets were applied. The enrichment analysis was completed for different tissues, since functional elements may differ across tissues. Enrichment outside the 99.9th percentile ($-\log_{10}$ binomial p value ≥ 3.38) was considered statistically significant (red in Fig. 2).

For Gene Ontology (GO) and functional enrichment analysis, the Database for Annotation, Visualization and Integrated Discovery (DAVID) v6.8 [44, 45], and the Enrichr [46, 47] tools were used. For GO analysis, DAVID v6.8 was used via the web interface (https://david.ncifcrf.gov/) using default settings. The gene lists corresponding to the top differentially methylated CpGs, the top differentially expressed transcripts from the RNAseq analysis, and top differentially expressed transcripts from the eQTM analysis (shown in Tables 2, 3, and 4, respectively) were used. Enrichr was also used via the web interface (https://maayanlab.cloud/Enrichr/), using the default settings and the whole genome set as background. The gene lists in Tables 2, 3, and 4 were used for Biological Process and Pathway enrichment. As output, results were exported from the GO Biological Process 2021 and the KEGG 2021 Pathways databases; p values are reported.

Abbreviations

CpGs	Cytosine-phosphate-guanine sites
DEG	Differentially expressed genes
DMC	Differentially methylated CpG
eQTM	Expression quantitative trait methylation
lcSSc	Limited cutaneous SSc
dcSSc	Diffuse cutaneous SSc
FDR	False discovery rate
SSc	Systemic sclerosis

Supplementary Information

The online version contains supplementary material available at https://doi.org/10.1186/s13148-023-01445-5.

Additional file 1. Supplementary Information.

Acknowledgements
The authors would like to acknowledge all the participants for their contribution to the study.

Author contributions
Conceptualization was contributed by PSR; Formal analysis was contributed by PCA, SS, DBF; Software was contributed by PCA; Investigation was contributed by PCA, SS, RCW, JRW, NHW, JF; Data curation was contributed by PCA; Visualization was contributed by PCA, SS, DBF; Resources were contributed by DMA, GSG, MAC; Supervision was contributed by DMA, MAC, CDL, PSR; Writing (original draft) was contributed by SS, PSR; Writing (review and editing) was contributed by SS, PCA, CDL, PSR. Project administration was contributed by PSR, DMA; Funding acquisition was contributed by PSR, GSG. All authors read and approved the final manuscript.

Funding
This work is supported by the US National Institute of Arthritis and Musculoskeletal and Skin Diseases of the National Institutes of Health (NIH) under Awards Number R03 AR065801 (PSR), P30 AR072582 (JF, GSG, PSR), P60 AR062755 (GSG, PSR), by the Scleroderma Foundation (PSR), the MUSC Center for Genomic Medicine (PSR), and the American College of Rheumatology Career Development Bridge Funding Award: K Bridge (DBF). Supported in part by the Cell Evaluation AND Therapy Shared Resource and by the Flow Cytometry and Cell Sorting Shared Resource, Hollings Cancer Center, Medical University of South Carolina (P30 CA138313).

Availability of data and materials
The gene expression and DNA methylation data presented in this study are openly available in the NCBI Gene Expression Omnibus (GEO) repository (Accession codes GSE196071 for the study, GSE196007 for the DNA methylation, and GSE196070 for the transcriptomic data). All data are also available from the authors on request. All code to reproduce these analyses are available at https://github.com/PeterCAllen/scleroderma_monocyte_analysis.

Declarations

Ethics approval and consent to participate
This study was approved by the Institutional Review Board at the Medical University of South Carolina (Pro# 33636). Informed consent was obtained from all participants. All research included in this manuscript conforms with the Declaration of Helsinki.

Consent for publication
Not applicable.

Competing interests
The authors declare that they have no competing interests.

Author details
[1]Department of Genetics, University of Alabama at Birmingham, Birmingham, AL, USA. [2]HudsonAlpha Institute for Biotechnology, Huntsville, AL, USA. [3]Department of Medicine, Medical University of South Carolina, Charleston, SC, USA. [4]Department of Pathology and Laboratory Medicine, Medical University of South Carolina, Charleston, SC, USA. [5]Department of Biostatistics and Data Science, Wake Forest University School of Medicine, Winston-Salem, NC, USA. [6]Center for Precision Medicine, Wake Forest University School of Medicine, Winston-Salem, NC, USA. [7]Department of Public Health Sciences, Medical University of South Carolina, Charleston, SC, USA.

Received: 6 April 2022 Accepted: 8 February 2023
Published online: 17 February 2023

References

1. Silver RM. Clinical aspects of systemic sclerosis (scleroderma). Ann Rheum Dis. 1991;50(Suppl 4):854–61.
2. Meier FM, Frommer KW, Dinser R, et al. Update on the profile of the EUSTAR cohort: an analysis of the EULAR Scleroderma Trials and Research group database. Ann Rheum Dis. 2012;71(8):1355–60.
3. Mayes MD, Lacey JV, Beebe-Dimmer J, et al. Prevalence, incidence, survival, and disease characteristics of systemic sclerosis in a large US population. Arthritis Rheum. 2003;48(8):2246–55.
4. Barnes J, Mayes MD. Epidemiology of systemic sclerosis: incidence, prevalence, survival, risk factors, malignancy, and environmental triggers. Curr Opin Rheumatol. 2012;24(2):165–70.
5. Ingegnoli F, Ughi N, Mihai C. Update on the epidemiology, risk factors, and disease outcomes of systemic sclerosis. Best Pract Res Clin Rheumatol. 2018;32(2):223–40.
6. Mendoza F, Derk CT. Systemic sclerosis mortality in the United States: 1999–2002 implications for patient care. J Clin Rheumatol Pract Rep Rheumatic Musculoskeletal Dis. 2007;13(4):187–92.
7. Laing TJ, Gillespie BW, Toth MB, et al. Racial differences in scleroderma among women in Michigan. Arth Rheum. 1997;40(4):734–42.
8. Greidinger EL, Flaherty KT, White B, et al. African-American race and antibodies to topoisomerase I are associated with increased severity of scleroderma lung disease. Chest. 1998;114(3):801–7.
9. Krishnan E, Furst DE. Systemic sclerosis mortality in the United States: 1979–1998. Eur J Epidemiol. 2005;20(10):855–61.
10. McNearney TA, Reveille JD, Fischbach M, et al. Pulmonary involvement in systemic sclerosis: associations with genetic, serologic, sociodemographic, and behavioral factors. Arth Rheum. 2007;57(2):318–26.
11. Nietert PJ, Mitchell HC, Bolster MB, et al. Racial variation in clinical and immunological manifestations of systemic sclerosis. J Rheumatol. 2006;33(2):263–8.
12. Morgan ND, Shah AA, Mayes MD, et al. Clinical and serological features of systemic sclerosis in a multicenter African American cohort: Analysis of the genome research in African American scleroderma patients clinical database. Medicine. 2017;96(51):e8980.
13. Ramos PS, Silver RM, Feghali-Bostwick CA. Genetics of systemic sclerosis: recent advances. Curr Opin Rheumatol. 2015;27(6):521–9.
14. Arnett FC, Cho M, Chatterjee S, et al. Familial occurrence frequencies and relative risks for systemic sclerosis (scleroderma) in three United States cohorts. Arth Rheum. 2001;44(6):1359–62.
15. Ramos PS, Zimmerman KD, Haddad S, et al. Integrative analysis of DNA methylation in discordant twins unveils distinct architectures of systemic sclerosis subsets. Clin Epigenetics. 2019;11(1):58.
16. Feghali-Bostwick C, Medsger TA, Wright TM. Analysis of systemic sclerosis in twins reveals low concordance for disease and high concordance for the presence of antinuclear antibodies. Arthritis Rheum. 2003;48(7):1956–63.
17. Ramos PS. Epigenetics of scleroderma: integrating genetic, ethnic, age, and environmental effects. J Scleroderma Relat Disorders. 2019;4(3):238–50.
18. Angiolilli C, Marut W, van der Kroef M, et al. New insights into the genetics and epigenetics of systemic sclerosis. Nat Rev Rheumatol. 2018;14(11):657–73.
19. Tsou PS, Varga J, O'Reilly S. Advances in epigenetics in systemic sclerosis: molecular mechanisms and therapeutic potential. Nat Rev Rheumatol. 2021;17(10):596–607.
20. Galanter JM, Gignoux CR, Oh SS, et al. Differential methylation between ethnic sub-groups reflects the effect of genetic ancestry and environmental exposures. Elife. 2017;6:e20532.

21. Matatiele P, Tikly M, Tarr G, et al. DNA methylation similarities in genes of black South Africans with systemic lupus erythematosus and systemic sclerosis. J Biomed Sci. 2015;22:34.
22. Baker Frost D, da Silveira W, Hazard ES, et al. Differential DNA methylation landscape in skin fibroblasts from african americans with systemic sclerosis. Genes. 2021;12(2):129.
23. Higashi-Kuwata N, Jinnin M, Makino T, et al. Characterization of monocyte/macrophage subsets in the skin and peripheral blood derived from patients with systemic sclerosis. Arth Res Ther. 2010;12(4):R128.
24. Kraling BM, Maul GG, Jimenez SA. Mononuclear cellular infiltrates in clinically involved skin from patients with systemic sclerosis of recent onset predominantly consist of monocytes/macrophages. Pathobiology. 1995;63(1):48–56.
25. van der Kroef M, van den Hoogen LL, Mertens JS, et al. Cytometry by time of flight identifies distinct signatures in patients with systemic sclerosis, systemic lupus erythematosus and Sjogrens syndrome. Eur J Immunol. 2020;50(1):119–29.
26. Toledo DM, Pioli PA. Macrophages in systemic sclerosis: novel insights and therapeutic implications. Curr Rheumatol Rep. 2019;21(7):31.
27. Quach H, Rotival M, Pothlichet J, et al. Genetic adaptation and neandertal admixture shaped the immune system of human populations. Cell. 2016;167(3):643-56e17.
28. Sharma S, Jin Z, Rosenzweig E, et al. Widely divergent transcriptional patterns between SLE patients of different ancestral backgrounds in sorted immune cell populations. J Autoimmun. 2015;60:51–8.
29. Reese C, Perry B, Heywood J, et al. Caveolin-1 deficiency may predispose African Americans to systemic sclerosis-related interstitial lung disease. Arth Rheumatol. 2014;66(7):1909–19.
30. Lee R, Reese C, Perry B, et al. Enhanced chemokine-receptor expression, function, and signaling in healthy African American and scleroderma-patient monocytes are regulated by caveolin-1. Fibrogenesis Tissue Repair. 2015;8:11.
31. Nedelec Y, Sanz J, Baharian G, et al. Genetic ancestry and natural selection drive population differences in immune responses to pathogens. Cell. 2016;167(3):657-69e21.
32. Menard LC, Habte S, Gonsiorek W, et al. B cells from African American lupus patients exhibit an activated phenotype. JCI insight. 2016;1(9):e87310.
33. Husquin LT, Rotival M, Fagny M, et al. Exploring the genetic basis of human population differences in DNA methylation and their causal impact on immune gene regulation. Genome Biol. 2018;19(1):222.
34. van der Kroef M, Castellucci M, Mokry M, et al. Histone modifications underlie monocyte dysregulation in patients with systemic sclerosis, underlining the treatment potential of epigenetic targeting. Ann Rheum Dis. 2019;78(4):529–38.
35. Ciechomska M, O'Reilly S, Przyborski S, et al. Histone demethylation and toll-like receptor 8-dependent cross-talk in monocytes promotes transdifferentiation of fibroblasts in systemic sclerosis via Fra-2. Arth Rheumatol. 2016;68(6):1493–504.
36. Arts RJW, Joosten LAB, Netea MG. The potential role of trained immunity in autoimmune and autoinflammatory disorders. Front Immunol. 2018;9:298.
37. Makinde HM, Dunn JLM, Gadhvi G, et al. Three distinct transcriptional profiles of monocytes associate with disease activity in scleroderma patients. Arth Rheumatol. 2022. https://doi.org/10.1002/art.42380.
38. van den Hoogen F, Khanna D, Fransen J, et al. 2013 classification criteria for systemic sclerosis: an American college of rheumatology/European league against rheumatism collaborative initiative. Ann Rheum Dis. 2013;72(11):1747–55.
39. Irish JC, Mills JN, Turner-Ivey B, et al. Amplification of WHSC1L1 regulates expression and estrogen-independent activation of ERalpha in SUM-44 breast cancer cells and is associated with ERalpha overexpression in breast cancer. Mol Oncol. 2016;10(6):850–65.
40. Hardiman G, Savage SJ, Hazard ES, et al. Systems analysis of the prostate transcriptome in African-American men compared with European-American men. Pharmacogenomics. 2016;17(10):1129–43.
41. Breeze CE, Paul DS, van Dongen J, et al. eFORGE: a tool for identifying cell type-specific signal in epigenomic data. Cell Rep. 2016;17(8):2137–50.
42. Breeze CE, Reynolds AP, van Dongen J, et al. eFORGE v2.0: updated analysis of cell type-specific signal in epigenomic data. Bioinformatics. 2019;35(22):4767–9.
43. Breeze CE, Haugen E, Reynolds A, et al. Integrative analysis of 3604 GWAS reveals multiple novel cell type-specific regulatory associations. Genome Biol. 2022;23(1):13.
44. da Huang W, Sherman BT, Lempicki RA. Bioinformatics enrichment tools: paths toward the comprehensive functional analysis of large gene lists. Nucleic Acids Res. 2009;37(1):1–13.
45. da Huang W, Sherman BT, Lempicki RA. Systematic and integrative analysis of large gene lists using DAVID bioinformatics resources. Nat Protoc. 2009;4(1):44–57.
46. Chen EY, Tan CM, Kou Y, et al. Enrichr: interactive and collaborative HTML5 gene list enrichment analysis tool. BMC Bioinform. 2013;14:128.
47. Kuleshov MV, Jones MR, Rouillard AD, et al. Enrichr: a comprehensive gene set enrichment analysis web server 2016 update. Nucleic Acids Res. 2016;44(W1):W90–7.
48. Selmi C, Feghali-Bostwick CA, Lleo A, et al. X chromosome gene methylation in peripheral lymphocytes from monozygotic twins discordant for scleroderma. Clin Exp Immunol. 2012;169(3):253–62.
49. Lian X, Xiao R, Hu X, et al. DNA demethylation of CD40l in CD4+ T cells from women with systemic sclerosis: a possible explanation for female susceptibility. Arthritis Rheum. 2012;64(7):2338–45.
50. Jiang H, Xiao R, Lian X, et al. Demethylation of TNFSF7 contributes to CD70 overexpression in CD4+ T cells from patients with systemic sclerosis. Clin Immunol. 2012;143(1):39–44.
51. Wang Y, Shu Y, Xiao Y, et al. Hypomethylation and overexpression of ITGAL (CD11a) in CD4(+) T cells in systemic sclerosis. Clin Epigenetics. 2014;6(1):25.
52. Wang YY, Wang Q, Sun XH, et al. DNA hypermethylation of the forkhead box protein 3 (FOXP3) promoter in CD4+ T cells of patients with systemic sclerosis. Br J Dermatol. 2014;171(1):39–47.
53. Li T, Ortiz-Fernández L, Andrés-León E, et al. Epigenomics and transcriptomics of systemic sclerosis CD4+ T cells reveal long-range dysregulation of key inflammatory pathways mediated by disease-associated susceptibility loci. Genome Med. 2020;12(1):81.
54. Samuel CE. Antiviral actions of interferons. Clin Microbiol Rev. 2001;14(4):778–809.
55. Drappier M, Sorgeloos F, Michiels T. The OAS/RNaseL pathway and its inhibition by viruses. Virologie. 2014;18(5):264–77.
56. Piera-Velazquez S, Mendoza FA, Addya S, et al. Increased expression of interferon regulated and antiviral response genes in CD31+/CD102+ lung microvascular endothelial cells from systemic sclerosis patients with end-stage interstitial lung disease. Clin Exp Rheumatol. 2021;39(6):1298–306.
57. Dumoitier N, Chaigne B, Regent A, et al. Scleroderma peripheral B lymphocytes secrete interleukin-6 and transforming growth factor beta and activate fibroblasts. Arth Rheumatol. 2017;69(5):1078–89.
58. Cao Z, Ge S, Xu Z, et al. beta3-Endonexin interacts with ninein in vascular endothelial cells to promote angiogenesis. Biochem Biophys Res Commun. 2021;566:75–9.
59. Howng SL, Chou AK, Lin CC, et al. Autoimmunity against hNinein, a human centrosomal protein, in patients with rheumatoid arthritis and systemic lupus erythematosus. Mol Med Rep. 2011;4(5):825–30.
60. Bergmann C, Akhmetshina A, Dees C, et al. Inhibition of glycogen synthase kinase 3beta induces dermal fibrosis by activation of the canonical Wnt pathway. Ann Rheum Dis. 2011;70(12):2191–8.
61. Grigoryev DN, Mathai SC, Fisher MR, et al. Identification of candidate genes in scleroderma-related pulmonary arterial hypertension. Transl Res. 2008;151(4):197–207.
62. Assassi S, Mayes MD, Arnett FC, et al. Systemic sclerosis and lupus: points in an interferon-mediated continuum. Arthritis Rheum. 2010;62(2):589–98.
63. Christmann RB, Hayes E, Pendergrass S, et al. Interferon and alternative activation of monocyte/macrophages in systemic sclerosis-associated pulmonary arterial hypertension. Arth Rheum. 2011;63(6):1718–28.
64. Hudson M, Bernatsky S, Colmegna I, et al. Novel insights into systemic autoimmune rheumatic diseases using shared molecular signatures and an integrative analysis. Epigenetics Offic J DNA Methyl Soc. 2017;12(6):433–40.

65. Bos CL, van Baarsen LG, Timmer TC, et al. Molecular subtypes of systemic sclerosis in association with anti-centromere antibodies and digital ulcers. Genes Immun. 2009;10(3):210–8.
66. Tan FK, Zhou X, Mayes MD, et al. Signatures of differentially regulated interferon gene expression and vasculotrophism in the peripheral blood cells of systemic sclerosis patients. Rheumatology. 2006;45(6):694–702.
67. York MR, Nagai T, Mangini AJ, et al. A macrophage marker, Siglec-1, is increased on circulating monocytes in patients with systemic sclerosis and induced by type I interferons and toll-like receptor agonists. Arthritis Rheum. 2007;56(3):1010–20.
68. Pendergrass SA, Hayes E, Farina G, et al. Limited systemic sclerosis patients with pulmonary arterial hypertension show biomarkers of inflammation and vascular injury. PLoS ONE. 2010;5(8):e12106.
69. Odani T, Yasuda S, Ota Y, et al. Up-regulated expression of HLA-DRB5 transcripts and high frequency of the HLA-DRB5*01:05 allele in scleroderma patients with interstitial lung disease. Rheumatology. 2012;51(10):1765–74.
70. Beretta L, Barturen G, Vigone B, et al. Genome-wide whole blood transcriptome profiling in a large European cohort of systemic sclerosis patients. Ann Rheum Dis. 2020;79(9):1218–26.
71. Moreno-Moral A, Bagnati M, Koturan S, et al. Changes in macrophage transcriptome associate with systemic sclerosis and mediate GSDMA contribution to disease risk. Ann Rheum Dis. 2018;77(4):596–601.
72. Assassi S, Wang X, Chen G, et al. Myeloablation followed by autologous stem cell transplantation normalises systemic sclerosis molecular signatures. Ann Rheum Dis. 2019;78(10):1371–8.
73. Dolcino M, Pelosi A, Fiore PF, et al. Gene profiling in patients with systemic sclerosis reveals the presence of oncogenic gene signatures. Front Immunol. 2018;9:449.
74. Farutin V, Kurtagic E, Pradines JR, et al. Multiomic study of skin, peripheral blood, and serum: is serum proteome a reflection of disease process at the end-organ level in systemic sclerosis? Arthritis Res Ther. 2021;23(1):259.
75. Gutierrez-Arcelus M, Lappalainen T, Montgomery SB, et al. Passive and active DNA methylation and the interplay with genetic variation in gene regulation. Elife. 2013;2:e00523.
76. Bonder MJ, Luijk R, Zhernakova DV, et al. Disease variants alter transcription factor levels and methylation of their binding sites. Nat Genet. 2017;49(1):131–8.
77. Bonder MJ, Kasela S, Kals M, et al. Genetic and epigenetic regulation of gene expression in fetal and adult human livers. BMC Genom. 2014;15:860.
78. Grundberg E, Meduri E, Sandling JK, et al. Global analysis of DNA methylation variation in adipose tissue from twins reveals links to disease-associated variants in distal regulatory elements. Am J Hum Genet. 2013;93(5):876–90.
79. Schubeler D. Function and information content of DNA methylation. Nature. 2015;517(7534):321–6.
80. Gutierrez-Arcelus M, Ongen H, Lappalainen T, et al. Tissue-specific effects of genetic and epigenetic variation on gene regulation and splicing. PLoS Genet. 2015;11(1):e1004958.
81. Ambrosi C, Manzo M, Baubec T. Dynamics and context-dependent roles of DNA methylation. J Mol Biol. 2017;429(10):1459–75.
82. O'Reilly S. Metabolic perturbations in systemic sclerosis. Curr Opin Rheumatol. 2022;34(1):91–4.
83. Michels KB, Binder AM, Dedeurwaerder S, et al. Recommendations for the design and analysis of epigenome-wide association studies. Nat Methods. 2013;10(10):949–55.
84. Barfield RT, Almli LM, Kilaru V, et al. Accounting for population stratification in DNA methylation studies. Genet Epidemiol. 2014;38(3):231–41.
85. Gopalan S, Carja O, Fagny M, et al. Trends in DNA methylation with age replicate across diverse human populations. Genetics. 2017;206(3):1659–74.
86. Fagny M, Patin E, MacIsaac JL, et al. The epigenomic landscape of African rainforest hunter-gatherers and farmers. Nat Commun. 2015;6:10047.
87. Heyn H, Moran S, Hernando-Herraez I, et al. DNA methylation contributes to natural human variation. Genome Res. 2013;23(9):1363–72.
88. Altorok N, Tsou PS, Coit P, et al. Genome-wide DNA methylation analysis in dermal fibroblasts from patients with diffuse and limited systemic sclerosis reveals common and subset-specific DNA methylation aberrancies. Ann Rheum Dis. 2015;74(8):1612–20.
89. Lu T, Klein KO, Colmegna I, et al. Whole-genome bisulfite sequencing in systemic sclerosis provides novel targets to understand disease pathogenesis. BMC Med Genom. 2019;12(1):144.
90. Helmick CG, Felson DT, Lawrence RC, et al. Estimates of the prevalence of arthritis and other rheumatic conditions in the United States. Part I Arth Rheum. 2008;58(1):15–25.
91. Volkmann ER, Tashkin DP, Sim M, et al. Short-term progression of interstitial lung disease in systemic sclerosis predicts long-term survival in two independent clinical trial cohorts. Ann Rheum Dis. 2019;78(1):122–30.
92. Volkmann ER, Steen V, Li N, et al. Racial disparities in systemic sclerosis: short- and long-term outcomes among African American participants of SLS I and II. ACR Open Rheumatol. 2021;3(1):8–16.
93. Ramos PS. Integrating genetic and social factors to understand health disparities in lupus. Curr Opin Rheumatol. 2021;33(6):598–604.
94. Johnson WE, Li C, Rabinovic A. Adjusting batch effects in microarray expression data using empirical Bayes methods. Biostatistics. 2007;8(1):118–27.
95. Absher DM, Li X, Waite LL, et al. Genome-wide DNA methylation analysis of systemic lupus erythematosus reveals persistent hypomethylation of interferon genes and compositional changes to CD4+ T-cell populations. PLoS Genet. 2013;9(8):e1003678.
96. Tian Y, Morris TJ, Webster AP, et al. ChAMP: updated methylation analysis pipeline for Illumina BeadChips. Bioinformatics. 2017;33(24):3982–4.
97. Nordlund J, Backlin CL, Wahlberg P, et al. Genome-wide signatures of differential DNA methylation in pediatric acute lymphoblastic leukemia. Genome Biol. 2013;14(9):r105.
98. Rahmani E, Shenhav L, Schweiger R, et al. Genome-wide methylation data mirror ancestry information. Epigenetics Chromatin. 2017;10:1.
99. Christiansen C, Castillo-Fernandez JE, Domingo-Relloso A, et al. Novel DNA methylation signatures of tobacco smoking with trans-ethnic effects. Clin Epigenetics. 2021;13(1):36.
100. R Development Core Team. R: A language and environment for statistical computing. Vienna, Austria: R Foundation for Statistical Computing; 2022.
101. Graw S, Henn R, Thompson JA, et al. pwrEWAS: a user-friendly tool for comprehensive power estimation for epigenome wide association studies (EWAS). BMC Bioinform. 2019;20(1):218.
102. Lund SP, Nettleton D, McCarthy DJ, et al. Detecting differential expression in RNA-sequence data using quasi-likelihood with shrunken dispersion estimates. Stat Appl Genet Mol Biol. 2012. https://doi.org/10.1515/1544-6115.1826.
103. Hart SN, Therneau TM, Zhang Y, et al. Calculating sample size estimates for RNA sequencing data. J Comput Biol. 2013;20(12):970–8.

Publisher's Note

Springer Nature remains neutral with regard to jurisdictional claims in published maps and institutional affiliations.

Ready to submit your research? Choose BMC and benefit from:

- fast, convenient online submission
- thorough peer review by experienced researchers in your field
- rapid publication on acceptance
- support for research data, including large and complex data types
- gold Open Access which fosters wider collaboration and increased citations
- maximum visibility for your research: over 100M website views per year

At BMC, research is always in progress.

Learn more biomedcentral.com/submissions